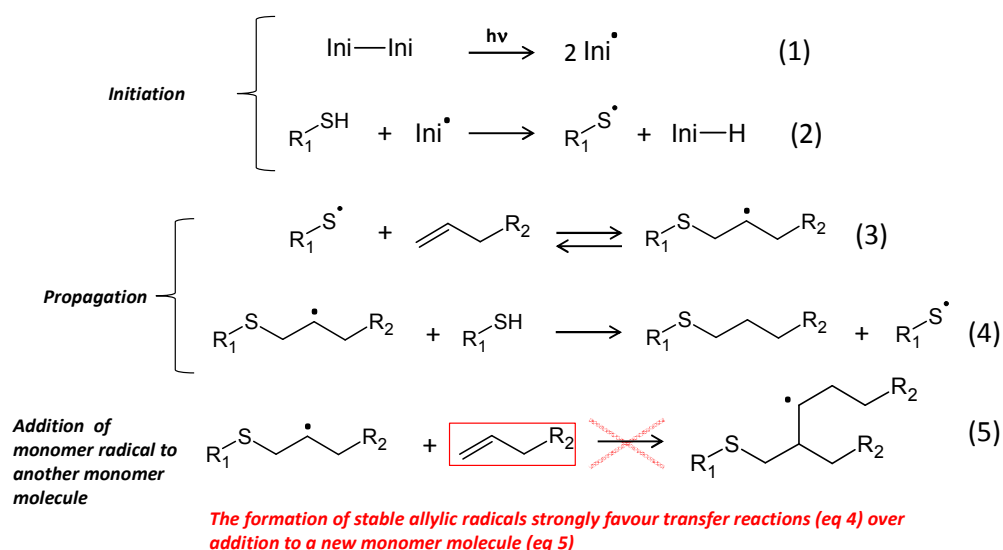


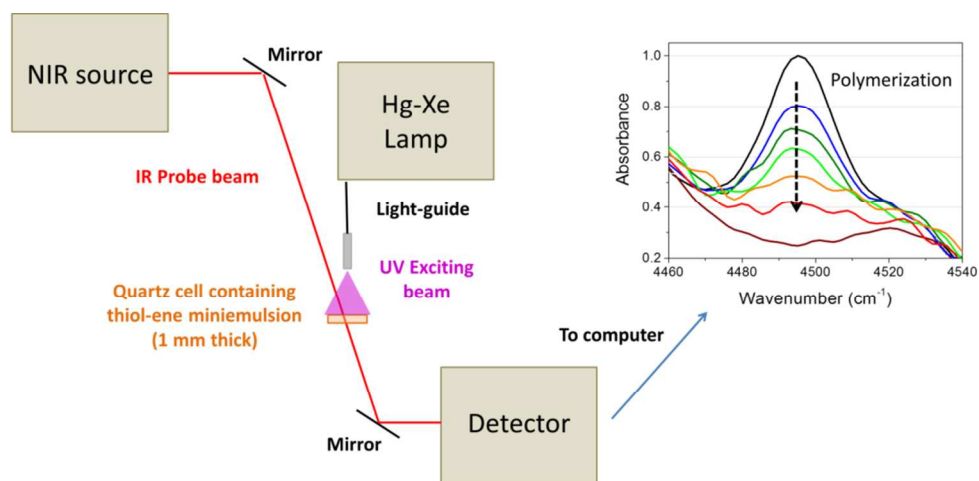
Supporting Information (SI)

Thiol-ene Linear Step-Growth Photopolymerization in Miniemulsion: Fast Rates, Redox-Responsive Particles, and Semi-Crystalline Films

Florent Jasinski, Agnès Rannée, Julie Schweitzer, Diane Fischer, Emeline Lobry, Abraham Chemtob, Céline Croutxé-Barghorn, Marc Schmutz, Didier Le Nouen, Adrien Criqui



Scheme S1. Mechanism of thiol-ene coupling reaction. Thiols can rapidly transfer a hydrogen atom to most types of photogenerated radical arising from a radical photoinitiator (eq 1-2, initiation). The resultant thiyl radical adds to the C=C bond to form a carbon-centered radical via a reversible process (eq 3, propagation step). The resulting radical can then abstract a hydrogen atom from another molecule of thiol to give the thioether product and a thiyl radical, which propagates the chain (eq 4, propagation step). A number of thiyl and carbon radical recombinations lead to termination.



Scheme S2. RT-FTNIR spectroscopy irradiation set-up for the online monitoring of reaction kinetics.

Table S1. Reproducibility experiments for the miniemulsions **M1**, **M2** and their resulting nanolatexes. Droplet and particle diameters were obtained by DLS. D_d were determined just after emulsification; and D_p after 20 s irradiation (nm). The size data are given in nm. The photopolymerizations were performed in a 1 mm thick spectroscopic cell under continuous light (filtered at 310 nm) provided by a mercury-xenon arc lamp ($\lambda = 310\text{-}600\text{ nm}$, $I = 590\text{ mW/cm}^2$).

Entry	Run 1 : D_d / D_p	Run 2 : D_d / D_p	Run 3 : D_d / D_p	Run 4 : D_d / D_p	Run 5 : D_d / D_p
M1 + 40 ppm DBHQ	163 / 165	158 / 162	160 / 158	159 / 164	145 / 140
M2 + 40 ppm DBHQ	153 / 163	192 / 171	156 / 158	193 / 182	156 / 183

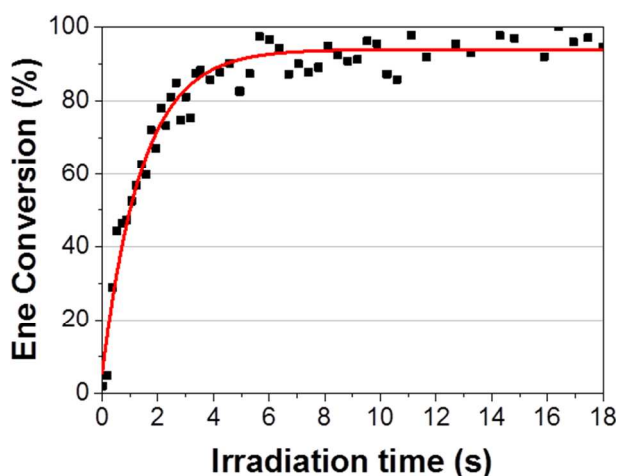


Figure S1. Experimental conversion vs time plot for thiol-ene miniemulsion photopolymerization were obtained by RT-FTNIR spectroscopy (■). Respective generated curve after fitting (red line). Sigmoidal functions Analytical solutions were used to fit the experimental data. Photopolymerization was performed in a 1 mm thick spectroscopic cell under continuous light (filtered at 310 nm) provided by a mercury-xenon medium pressure arc lamp. $D_d = 150\text{ nm}$, $C_{\text{monomer}} = 20\text{ wt \%}$.

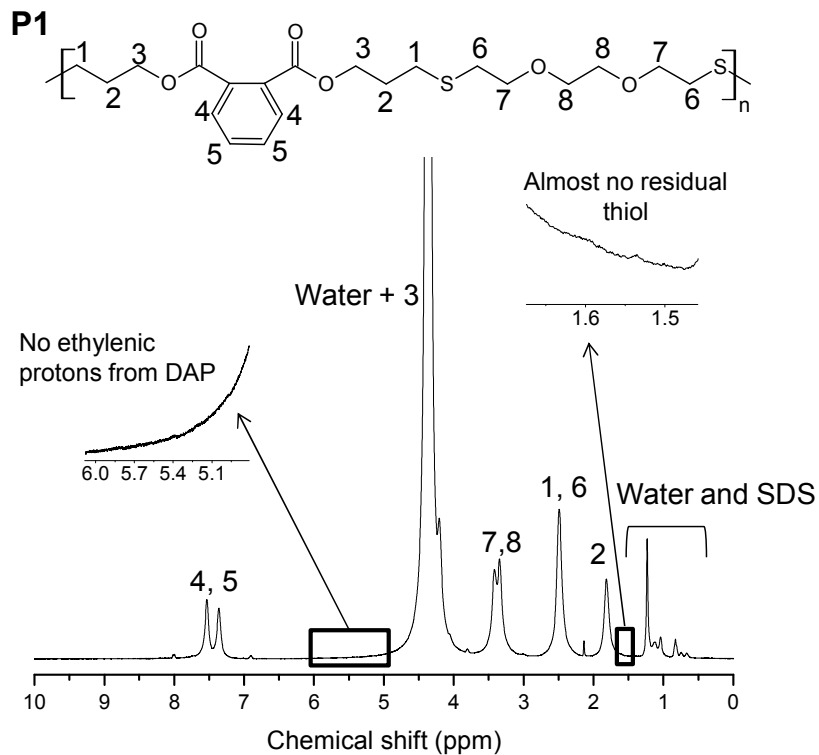


Figure S2. Online detection of ene conversion in **P1** by ^1H NMR spectrum performed at 60°C . The H_2O broad signal at 4.20 ppm dominates the spectrum as expected. However, the olefinic (5 - 6 ppm) and thiol (1.5 - 1.6 ppm) regions are sufficiently resolved to detect the presence of residual end chains. Ethylenic protons signals from **DAP** (5.25 ppm and 5.90 ppm) or thiol protons resonances from **EDDT** (1.55 ppm) vanished below the noise level.

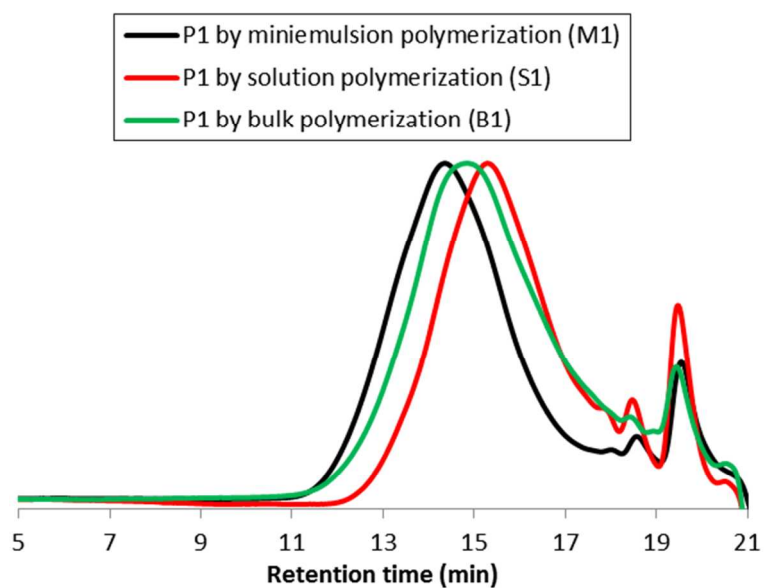


Figure S3. SEC traces of **P1** produced by photopolymerization in miniemulsion (**M1**, black line), bulk (**B1**, green line) and solution (**S1**, red line) in DMSO. Photopolymerization was performed in a 1 mm thick spectroscopic cell under continuous light (filtered at 310 nm) provided by a mercury-xenon medium pressure arc lamp at $C_{\text{monomer}} = 20$ wt %.

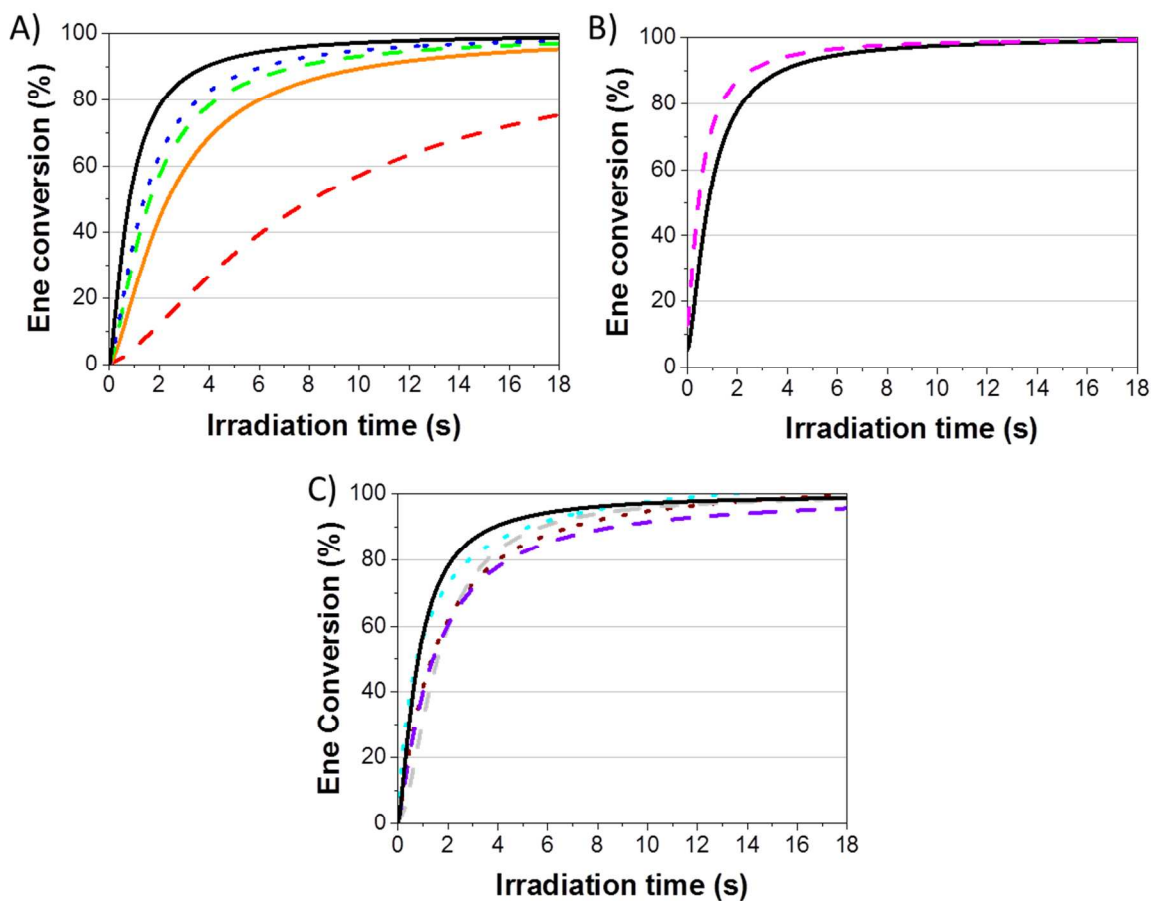


Figure S4. Effect of various parameters on conversion vs time curves profiles for EDDT-DAP miniemulsion photopolymerization. All photopolymerizations were performed in a 1 mm thick spectroscopic cell under continuous light (filtered at 310 nm) provided by a mercury-xenon medium pressure arc lamp. $D_d = 150$ nm, $C_{\text{monomer}} = 20$ wt %

A) Irradiance effect: $\lambda = 310\text{-}600$ nm, $I = 590$ mW cm⁻² (black line), 294 mW cm⁻² (blue dotted line), 235 mW cm⁻² (green dashed line), 147 mW cm⁻² (orange line), 60 mW cm⁻² (red dashed line), $PI = I2959$.

B) PI effect: I651 (purple dashed line), I2959 (black line), $I = 590$ mW cm⁻².

C) Monomer content effect: $C_{\text{monomer}} = 20$ wt % (black line), 25 wt % (light grey dashed line), 30 wt % (violet dashed line), 35 wt % (light blue line), 50 wt % (brown dotted line), $I = 590$ mW cm⁻², $PI = I2959$.

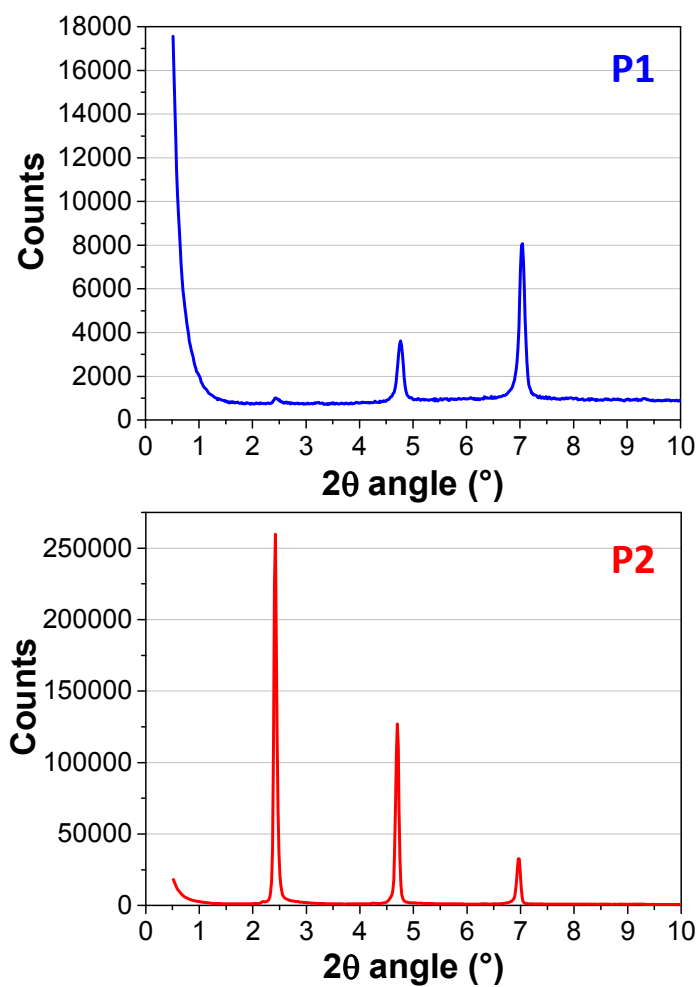


Figure S5. Small-angle XRD patterns of **P1** and **P2** films

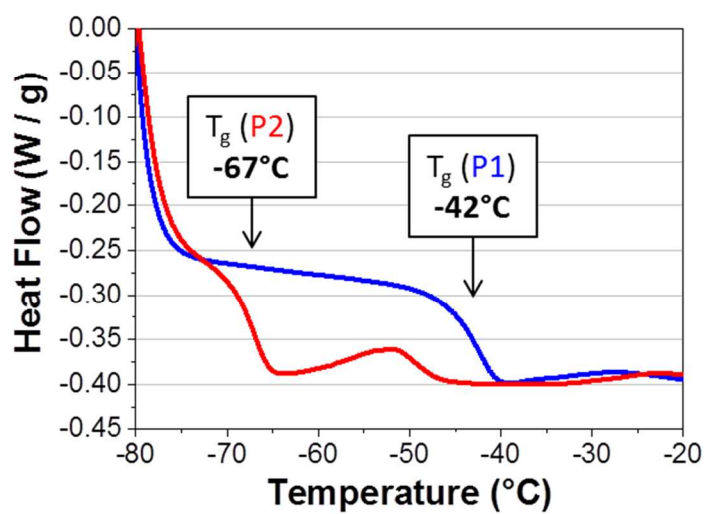


Figure S6. DSC thermograms of **P1** and **P2** films in the region between -80°C and -20°C showing the glass transitions

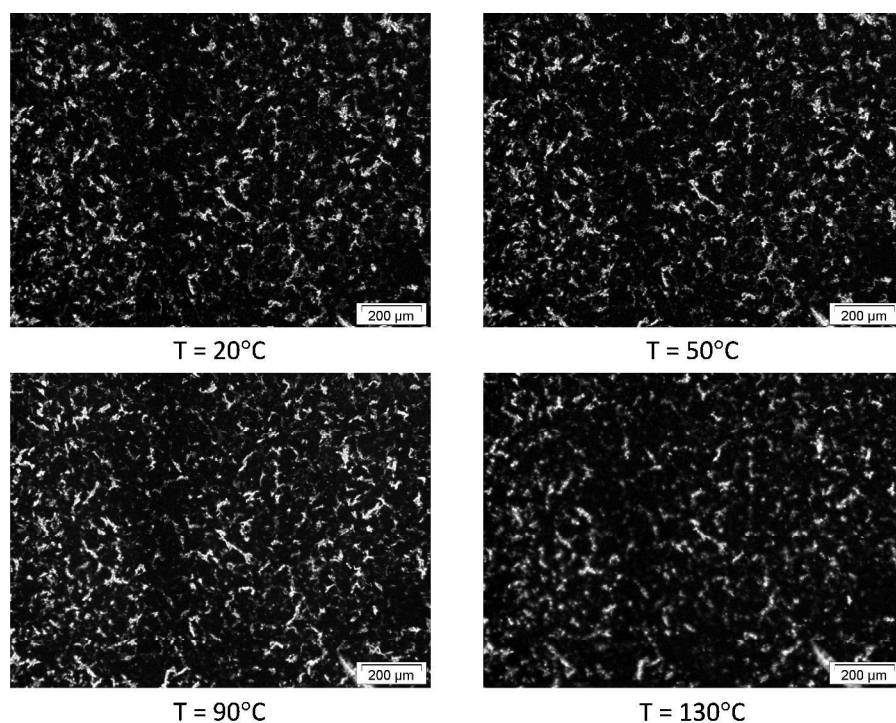


Figure S7. Series of POM images of the polysulfide film derived from P2 and taken at different temperatures

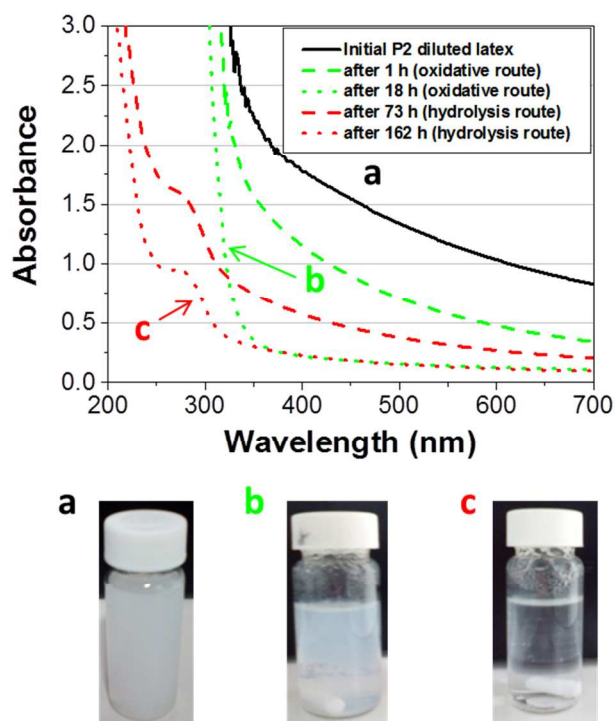


Figure S8. UV-Visible absorbance spectra of diluted P2 latex over time, under oxidative and acid hydrolysis stress.